Chemical Engineering & Processing: Process Intensification 205 (2024) 109975

Contents lists available at ScienceDirect

Chemical Engineering and Processing - Process Intensification

journal homepage: www.elsevier.com/locate/cep

Design and optimisation of lysozyme protein purification process using non-thermal progressive freeze concentration technology

Tazien Rashid [a,b,c], Mazura Jusoh [d,e,*], Zaki Yamani Zakaria [e], Norshafika Yahya [e], Sabah Ansar [f], Tiong Sieh Kiong [b], Farooq Sher [g,*]

[a] School of Engineering and Physical Sciences, Heriot-Watt University, Dubai P.O. Box 501745, United Arab Emirates
[b] Institute of Sustainable Energy (ISE), Universiti Tenaga Nasional, Selangor 43000, Malaysia
[c] Research Centre for Marine and Land Bioindustry, National Research and Innovation Agency (BRIN), North Lombok Regency, West Nusa Tenggara 83352, Indonesia
[d] Faculty of Chemical and Energy Engineering, Universiti Teknologi Malaysia, Johor Bahru, Johor 81310, Malaysia
[e] Centre of Lipid Engineering and Applied Research (CLEAR), Universiti Teknologi Malaysia, Johor Bahru, Johor 81310, Malaysia
[f] Department of Clinical Laboratory Sciences, College of Applied Medical Sciences, King Saud University, P.O. Box 10219, Riyadh 11433, Saudi Arabia
[g] Department of Engineering, School of Science and Technology, Nottingham Trent University, Nottingham NG11 8NS, United Kingdom

ARTICLE INFO

Keywords:
Multiple probe cryo-concentrator
Sustainable
Lysozyme protein
Biochemical engineering
Non-thermal
Sustainable food production and energy efficiency

ABSTRACT

In this study, PFC system is investigated to improve the concentration and yield of lysozyme. The research focused on an attempt to thoroughly construct an ice crystallizer with measurable and optimized design parameters for an efficient lysozyme protein concentration procedure because the productivity of PFC is always an issue. A new Multiple Probe Cryo-Concentrator (MPCC) device was designed and successfully equipped with probes having a well-distributed cooled surface area for ice crystallization with proper internal cooling temperature control as well as a solution movement mechanism provided by a stirrer in the tank. The impact of different operating parameters is optimally investigated. Central Composite Design (CCD) is utilized to optimize PFC operating conditions and their response to partition constant (K-value) and solute yield. The results showed that a coolant temperature of -12 ºC, stirrer speed of 350 rpm, operation time of 40 min and initial concentration of 10 mg/mL gave the best K-value (0.132) and solute concentration yield (87.39 %). The design elements of the equipment are crucial in providing improved PFC performance. The study revealed that the PFC system designed and applied in this study can improve the lysozyme protein concentration as needed in the food and pharmaceutical industry.

1. Introduction

Lysozyme is an antibacterial peptide with high enzymatic activity and positive charges. It has been used as an antibacterial agent in the food and pharmaceutical industries. The most abundant and readily available type of lysozyme in the market is egg-white lysozyme [1]. The need for purified proteins is currently growing, particularly for applications in the culinary, biochemical and pharmaceutical industries, with fewer or no shortcomings. To study and analyse the adaptability, economic aspect, simplicity, along with high quality and quantity of lysozyme concentration various researchers on a laboratory scale and industrial experts on an industrial scale developed and refined lysozyme purification technologies from hen egg white. There are about three different strategies that prior researchers have recommended [2].

Ultrafiltration, dialysis, precipitation, and chromatography are a few of them. However, due to its ease of use, the freeze concentration approach has recently caught the attention of researchers in lysozyme purification. Table 1 lists earlier technologies that have been investigated by researchers in the past until now. Looking at the disadvantages of other methods, this study suggests concentrating lysozyme using gradual freeze concentration method. Freeze concentration works by turning the water in a solution into ice crystals, in doing so the solution is concentrated. In addition to creating a concentrate of high-quality freeze concentration has various advantages as compared to evaporation and membrane technology. The process takes place at a low temperature where there is no vapour-liquid interface and hence no volatile losses [2]. Due to the less complicated separation process, industrial freeze concentration has recently been developed based on a one-step

* Corresponding authors.
E-mail addresses: mazura@cheme.utm.my (M. Jusoh), Farooq.Sher@ntu.ac.uk (F. Sher).

https://doi.org/10.1016/j.cep.2024.109975
Received 1 December 2023; Received in revised form 15 July 2024; Accepted 2 September 2024
Available online 6 September 2024

Table 1
Comparison of progressive freeze concentration technologies used in the literature.

Method	Type	Results	Disadvantages	Year	Reference
Precipitation	Alcohol extraction	Fresh yield: 54.4 % Dried yield: 89 %	More alcohol; partial loss of lysozyme activity; reduced recovery of lysozyme	2010	[56]
Aqueous two-phase system	Thermoseparating random copolymer	Yield: 85 % Lysozyme Concentration= 2.3 g/l	High cost of materials; low purity of lysozyme	2010	[57]
Ion-exchange chromatography	Anion-exchange chromatography + chromatographic separation	Yield: 70 %	Long times required; low capacity; complicated reactions and equipment.	2010	[58]
Multi-method	Direct crystallization, ion-exchange chromatography and ultrafiltration methods	Ion-exchange chromatography: effect isolation = 70 −85 % Ultrafiltration: effect isolation = 15–20 %	Long time required	2012	[59]
Ion-exchange chromatography	Natrixadsept TM weak cation-exchange membranes (+hydrogel layer attached to a polymer matrix)	Protein concentration ethanol soluble egg white= 36.9 % in pure Lysozyme= 85.7 %	Long times required Low capacity	2012	[60]
Ion-exchange chromatography	Amberlite FPC 3500 ion-exchange resin	Final lysozyme= 88.90 ± 1.93	Long times required Low capacity	2013	[61]
Ion-exchange chromatography	FPC3500 cation-exchange resin, the sequential separation method	Laboratory scale 289 g of egg white= 89.72 ± 1.93 % Large scale 3625 g of egg white = 88.72 ± 3.61 %	Long times required Low capacity	2014	[62]
Freeze concentration	Yield = 51.8 % Time= more than an hour	Double wall beaker with one finger probe and separation method used centrifugation	More time consumption Less of production Less increment yield	2014	[42]
Multi-method	Lysozyme partially purified egg white lysozyme extracted from kampong chicken= 5800 μg/mL Cihateup duck= 5500 μg/mL Commercial laying hens= 5400 μg/mL	Ethanol precipitation + ion exchange chromatography	Contaminate with ethanol solution	2015	[63]
Dialysis	Removal rates of lysozyme were significantly lower in BPA-coated: p-value=0.22	Eight polymer membrane columns with four of them were coated with a BPA product	Limitation study because lysozyme is adsorbed by several polymers only	2017	[64]
Ultrafiltration	Best membrane polymer concentration = 19 % w/w Yield lysozyme = 97 %	Membrane solutions with different polymer concentration of Polyehtersulfone/N–Methyl pyrolidone/water	High maintenance due to clogging pores	2017	[65]
Dialysis	Macroscopic ultrathin protein membrane		More time required (4 h) High maintenance of replacement membrane	2018	[66]
Ultrafiltration	High flow velocity Transmembrane pressure Time= 5 h	Tubular UF membrane with ceramic membrane, composed of a galumina support and an active layer of TiO2, with an asymmetric pore structure	High maintenance due to clogging pores Long time consuming	2019	[67]

system, which is PFC, as compared to conventional freeze concentration. The PFC is built on a similar idea but it grows a single larger ice mass that forms and grows on the chilled exterior, simplifying the process of separation from the mother solution. This facilitates the liquid's separation from the concentrated liquid on the ice block's cooled surface [3]. To achieve high-end product concentration and reduce operation time for subcutaneous delivery, there are various significant obstacles [4].

Other concentration methods like reverse osmosis and evaporation have some drawbacks as well as benefits, such as the high processing cost of achieving the required osmotic pressure and for replacing damaged membranes brought on by clogging, the high energy requirements, and the risk of biological structure destruction from the high temperatures used. All of the issues and drawbacks may result in a decrease in the quality of the protein, and occasionally inadequate production of highly concentrated protein. It is crucial to overcome these significant obstacles to enable a successful operation of PFC process for lysozyme protein concentration [5]. To boost productivity and provide the ideal environment for the most efficient lysozyme concentration using a non-thermal process, the goal of the present research relies on building a new ice crystallizer based on progressive freeze concentration phenomenon with optimized design parameters. In PFC, the development of an ice crystal lattice should potentially reject all contaminants to form highly pure ice, leaving behind an increased concentration of protein solution. Additionally, molecule size has little impact on the PFC process [6]. Literature shows that this procedure for protein concentration is not being employed to date. To propose a new method of achieving the desired concentration of protein solution, it is crucial to analyse the impact of process conditions on protein concentration.

To improve the existing methods of lysozyme concentration, the purpose of this study is to search for a novel alternative method. Consequently, a new piece of equipment was fabricated having a set of multiple probes for ice crystallisation and named as multiple probe cryoconcentrator (MPCC). The newly designed probes maximize the surface area available for interaction between the solution and the cooled surface. The surface area offered by MPCC was compared with the traditional PFC arrangement to objectively evaluate this study. Although MPCC has been reported to concentrate cucumber juice, however, it is important to observe the capability of the same apparatus to handle a more sensitive material such as lysozyme [7]. This study aims to ascertain the effects of multiple process variables on the partition constant (K-value), solute concentration yield (%), concentration index (CI), and average ice growth rate (ice) of lysozyme protein concentrate. These variables include coolant temperature (°C), operation time (min), stirrer speed (rpm), and initial concentration (mg/mL). Optimization of protein concentration process has been performed in previous literature [8-10]. Ekpeni et al., [8] employed response surface methodology (RSM) to optimize protein concentration yield from homogenized baker's yeast. Similarly, Szerman et al., [9] performed RSM to increase the efficiency of whey protein concentration.

Following the design features investigated, RSM is used to determine the best operating parameters for the coolant temperature (ºC), operation time (min), stirrer speed (rpm) and initial concentration to achieve the designed MPCC system's best performance. The choice of technology utilised in the protein concentration process is crucial for maintaining the method's effectiveness, efficiency, and affordability. In addition to providing a PFC process with a more efficient heat transfer phenomenon, this newly developed MPCC intensifies the protein purification

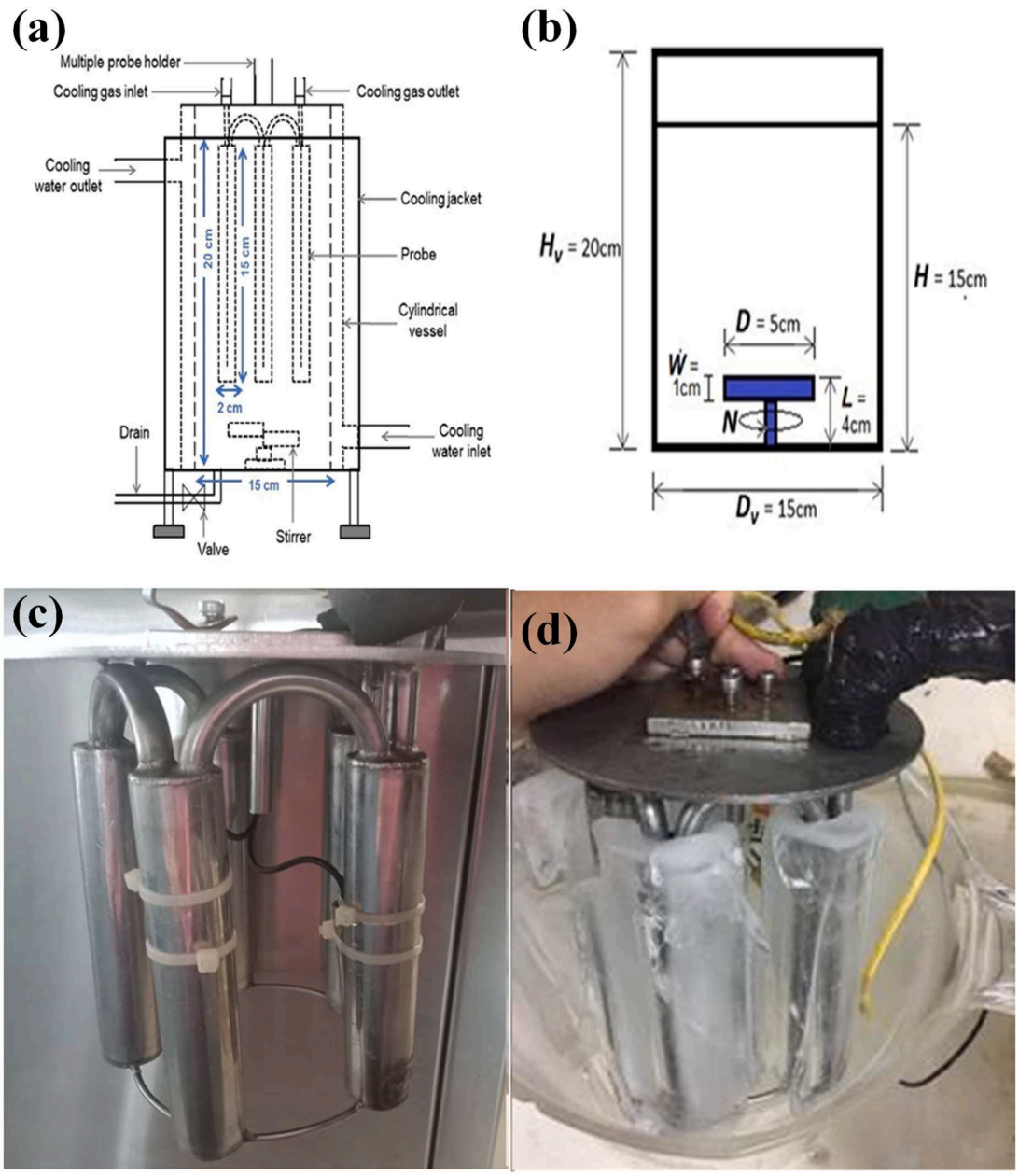

Fig. 1. (a) Schematic diagram of multiple probe cryo-concentration system, (b) Dimensions of the stirrer and solution tank, (c) Progressive freeze concentration using MPCC concentrator and (d) Fabrication of progressive freeze with MPCC concentrator.

technique as it can be proven from this work to be a useful advanced process in carrying out lysozyme concentration that could ensure no volatile loss and preserve the protein quality as it can be conducted at a sub-zero temperature.

2. Materials and methods

2.1. Materials

As a model for a protein antibody solution, lysozyme from chicken egg white powder (crystalline), CAS number 12,650–88–3 was purchased from Sigma-Aldrich (M) Sdn. Bhd. to form the solution. In the water bath, water mixed with 50 % ethylene glycol (purchased from Sigma-Aldrich) was utilised as the solution coolant medium placed in the jacket of the cylindrical vessel. The freezing point of ethylene glycol-water cooling medium depends very largely on its percentage with water and at 50 %, the freezing point is brought down to −37 °C. R22 gas was employed in the probe cooling system (Embraco, Brazil) which has a 464 W cooling capacity with the capability to bring the temperature down to −10 to −20 °C.

2.2. Construction of multiple probe cryo-concentrator (MPCC)

This work engaged MPCC as the main apparatus for the PFC approach. The design is inspired by ice crystallization technology [11]. The apparatus, which consists of a cylindrical stainless-steel tank with a 3200 mL capacity, an internal diameter of 15 cm, a height of 20 cm, and a thickness of 0.1 cm, is designed as depicted in Fig. 1(a) and (b). The target solution was injected into the cylindrical vessel, where ice crystallisation was used to accomplish the separation procedure. At the bottom of the tank is a motor-operated stirrer with a variable speed that is used to manage the rate of movement of the ice front and solute [12]. The stainless-steel probe with five fingers (called probes) that is shown in Fig. 1(c) has a hollow interior that is filled with coolant gas (R22).

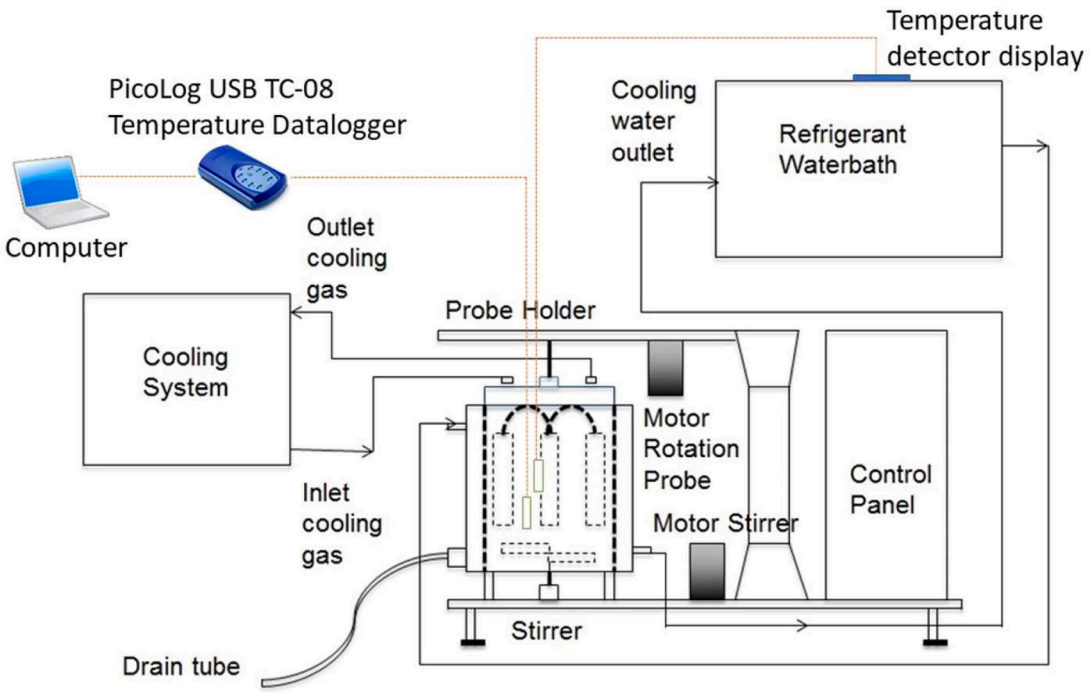

Fig. 2. Process flow diagram of experimental setup along with different instruments and components.

Through appropriate copper tubing and direct supply to the probe that was submerged in the solution tank, this refrigerant system cools the solution [12,13]. The five-probe set was created as shown in Fig. 1(c) to be able to spin at 180° inter-defectively while stirring it at a speed that will optimize the production of ice on the probe's exterior and ensure that the solution is well mixed. To prevent the solution's heat from transferring, the cylindrical vessel's exterior is covered in a coolant jacket made of polyurethane foam. In addition, a space between the cylindrical vessel and the coolant jacket has a space for ethylene glycol-water coolant solution that is supplied directly from the water bath to maintain the solution's temperature around the freezing point of pure water (2 °C).

2.3. Experimental procedure

Firstly, the lysozyme solution was prepared by dissolving the powder in water to achieve a range of initial concentrations to be investigated. This is to cater for the real food and pharmaceutical industry where the lysozyme solution can be in various concentrations before it can be concentrated for further processes and products. The UV–Vis spectrophotometer (UV-mini-1240, Shimadzu, Japan) was used to measure the starting concentrations in this investigation, which ranged from 6 to 14 mg/mL at a wavelength of 280 nm. The lysozyme solution was introduced into the cylindrical tank and allowed to cool until it approached the freezing point of pure water (2 °C). This allowed the ice crystallisation process to begin in the PFC experiment. The volume capacity of the tank is 3200 mL and continuously supplied with the ethylene glycol-water solution in the jacket to maintain the temperature at 2 °C. To start the PFC process, the stirrer in the tank was set to the preferred speed (200 to 400 rpm) to provide movement for the lysozyme solution to facilitate optimal ice formation on the exterior surface of the probes and assist solute separation [12].

The probes were then placed inside the cylindrical vessel containing the lysozyme solution and instructed to rotate 180°. The cylindrical vessel was ensured to be airtight to stop heat from escaping into the environment. The temperature of the coolant gas was adjusted to the required range (−14 to −6 °C) [14]. The stopwatch was started as soon as the target temperature was achieved, marking the beginning of operation time (20 to 60 min). A thermocouple (type-K) data logger (PicoLog USB TC-08 with Development Kit Linux software, made by Pico Technology United Kingdom and acquired from RS Components (M) Sdn. Bhd.) was used to track the temperature of the solution inside the cylindrical vessel. The data logger continuously presented this information online for a simple process of monitoring. Fig. 2 represents the schematic of the process experimental setup. The cryo-concentration procedure was stopped once the intended time frame was finished. The multiple probes were then set aside of the vessel and thickening of the ice layer was observed on the probe fingers. The remaining solution (concentrated) was drained and the ice crystals formed were immediately collected as samples. The trials were then repeated with varied operational parameter values, with only one parameter changing per iteration while the others were maintained fixed. Using a UV–vis spectrophotometer, the contents of lysozyme were determined in both concentrated and thawed solutions.

2.4. Design of experiment

The experimental setup was used to optimize partition constant (K-value) and solute concentration yield of lysozyme and to develop a procedure that is sustainable and energy-efficient. The variables are coolant temperature (−16, −14, −12, −10 and −8 °C), operation time (20, 30, 40, 50 and 60 min), stirrer speed (250, 300, 350, 400 and 450 rpm) and initial lysozyme concentration (6, 8, 10, 12 and 14 mg/mL) respectively. For the studied parameters the partition constant (K- value) and solute concentration yield were calculated as responses.

2.5. Determination of protein concentration

Using a UV–vis spectrophotometer, the absorbance of a sample of lysozyme solution was measured to calculate the protein concentration in the sample [15]. For each run, a concentrated lysozyme sample (sample 1) and an ice sample (sample 2) were taken and then examined to determine the lysozyme protein absorbance. The protein concentration was measured based on a calibration curve constructed using bovine serum albumin (BSA). BSA samples were kept in the freezer for preservation before being used and then mixed with chilled acetone at a

1:5 ratio in a test tube. This test tube was then centrifuged for 35 min at 2500 rpm. After the centrifugation, an additional 5 mL of chilled acetone was added to the sample. This sample was again centrifuged at 2500 rpm for an additional interval of 10 min. After centrifugation, the material was then examined for its protein concentration for calibration purposes.

2.6. Evaluation of process behaviour and system efficiency

Using Eq. (1) to analyse the behaviour of the FC process, the effective partition constant (K-value) was calculated to identify the effect of variables on the FC experimental data [16]. Where CL and CO represent the lysozyme concentrations in the concentrated and starting solution in g/mL, and VL and VO represent the volume of the concentrated and original solution in millilitres [17]. The MPCC system's design is focused on the concentration process. It is thought that solute recovery, Y, is required to assess the solute concentration yield. Solutes should be fully rejected from the developing ice crystal to achieve the ideal concentration rate. However, depending on the experimental circumstances, the solutes might be stuck in the ice crystal. Following Eq. (2) is used to define solute concentration Y (%) [18].

$$K = 1 - \frac{\log \frac{C_O}{C_L}}{\log \frac{V_L}{V_O}} \tag{1}$$

$$Y = \frac{C_L}{C_O}\frac{m_L}{m_o} \tag{2}$$

where m_L and m_O are the mass of the concentrated and initial solution in g. At the end of the PFC procedure, the concentration index (CI) was calculated to assess the effects of an operating parameter or variable. The link between an aqueous solution's initial and final concentrations is also shown. This relationship can be studied using the following Eq. (3) [16]. Where Xs liq is the solute concentration in the liquid (mg/mL), Xso is the starting concentration (mg/mL), and CI is the concentration index. To ensure excellent quality and concentration in the product, kinetics is one of the top priorities in the PFC process. The kinetics of the solution is determined by the growing rate of ice crystals on the coolant wall [19,20]. When the heat of crystallisation travels over the solution towards the wall, a conductive heat transfer resistance is created (Ehrlich et al., 2015) Eq. (4) can be utilized to calculate the average ice growth rate $\tilde{v}_{ice}$ provided that the limiting factor is heat transfer [21].

$$CI = \frac{X_{s\ liq}}{X_{s\ o}} \tag{3}$$

$$Y = \beta o + \beta 1X1 + \beta 2X2 + \beta 3X3 + \beta 4X4 + \beta 12X1X2 + \beta 13X1X3 + \beta 14X1X4 + \beta 23X2X + \beta 24X2X4 + \beta 34X3X4 + \beta 11X12 + \beta 22X22 + \beta 33X32 + \beta 44X42 \tag{6}$$

$$\tilde{v}_{ice} = \frac{m_{T.ice}}{A\tau\rho_{ice}}(1 - \omega_{s.ice})(10^6) \tag{4}$$

$$\omega_{s.ice} = \frac{m_s}{m_T} \tag{5}$$

where ρ_{ice} is the density of pure ice (kg/m^3), A is the area covered by ice on the probe's wall (m^2), $m_{T.ice}$ is the mass of melted ice-water (kg), τ is the length of time the experiment was run (s), and ωs ice is the solute mass fraction (kg/kg) as given by Eq. (5) [22]. Where m_s is the mass of solute in the melted ice-water (kg) and m_T is the mass of total ice. The time, flow rate and speed of the stirrer determine whether the procedure of the crystalliser can be used to achieve an effective ice growth rate. The findings of this study will make it possible to comprehend ice crystal formation processes and phenomena at cooled surfaces in crystallisation processes with clarity. Additionally, a simplified crystallizer design using a straightforward heat exchanger is presented. This design will serve as the foundation for future advancements in the progressive freeze concentration concept separation.

Table 2
Experimental range and levels of variables selected for central composite design (CCD) used to study effective partition constant and solute concentration yield.

Parameter	Symbol	-α	−1	0	+1	+α
Coolant temperature (°C)	X_1	−16	−14	−12	−10	−8
Operation time (min)	X_2	20	30	40	50	60
Stirrer speed (rpm)	X_3	250	300	350	400	450
Initial concentration (mg/mL)	X_4	6	8	10	12	14

2.7. Statistical analysis

A central composite design was used to study the effects of four operating parameters on lysozyme concentration towards K-value and solute yield (Y (%)), namely coolant temperature X1 (°C), operation time X2 (min), stirrer speed X3 (rpm), and initial concentration X4 (mg/mL), based on the preliminary experimentation results obtained. To select the range of parameters for this study preliminary screening experiments were performed. The arrangement of experiments is shown in Table 3 and Table 4 respectively. The trials were carried out individually, and the software recommended 26 runs at five levels with two repetitions and an axial point (at selected α = 2.0). Based on initial screening experiments the central composite design (CCD) was used to evaluate two responses of K-value and solute yield as shown in Table 2.

2.8. Optimization process

The optimization of operating parameters including coolant temperature X_1 (°C), operation time X_2 (min), stirrer speed X_3 (rpm) and initial concentration X_4 (mg/mL) towards K-value and solute concentration yield was investigated using RSM tool using Statgraphics Centurion15.2.11.0 version 8.0 [23]. The most popular fractional factorial design in RSM was employed called the Central Composite Design (CCD) which is widely used to identify certain optimum value combinations and to associate the K-Value and solute yield to other independent variables, with the regression model [24] as shown in the following equation (Eq. (6)).

where Y is the response value predicted, β_0 is the regression constant, β_1, β_2, β_k are the coefficients of regression. Design Expert software (version 6.0.4, Stat-Ease, Inc.) was utilized to calculate the regression model for the predicted response, and statistical analysis of the data, also the adequacy of the model was checked for future predictions. Based on the Design of Experiments (DOE) an experimental design was built where X_1, X_2, X_3 and X_4 are termed as independent variables. Table 2 displays the low, middle and high levels for all the parameters. The central composite design (CCD) was used to perform the extreme measures and presented by –α and +α which are shown in Table 2. The CCD design

Table 3
Experimental design matrix based on CCD for effective partition constant.

Run	Coolant temperature	Operation time	Stirrer speed	Initial concentration	K-Value	
	X_1 (°C)	X_2 (min)	X_3 (rpm)	X_4 (mg/mL)	Experimental	Predicted
1	−10	30	400	8	0.140	0.132
2	−8	40	350	10	0.301	0.226
3	−12	40	350	10	0.140	0.140
4	−12	40	350	6	0.042	0.012
5	−12	40	350	14	0.099	0.075
6	−16	40	350	10	0.540	0.561
7	−10	50	400	12	0.062	0.087
8	−12	40	250	10	0.390	0.370
9	−10	50	400	8	0.130	0.164
10	−10	30	300	8	0.070	0.127
11	−14	30	400	8	0.190	0.227
12	−10	50	300	8	0.201	0.219
13	−14	50	400	8	0.281	0.277
14	−14	30	400	12	0.344	0.336
15	−12	20	350	10	0.216	0.171
16	−12	40	350	10	0.141	0.140
17	−10	30	300	12	0.160	0.174
18	−10	50	300	12	0.172	0.173
19	−12	60	350	10	0.231	0.221
20	−12	40	450	10	0.29	0.256
21	−14	50	400	12	0.31	0.293
22	−14	30	300	8	0.27	0.256
23	−14	50	300	12	0.394	0.413
24	−10	30	400	12	0.094	0.148
25	−14	50	300	8	0.381	0.366
26	−14	30	300	12	0.39	0.396

Table 4
Experimental design matrix based on CCD for solute concentration yield.

Run	Coolant temperature	Operation time	Stirrer speed	Initial concentration	Yield (%)	
	X_1 (°C)	X_2 (min)	X_3 (rpm)	X_4 (mg/mL)	Experimental	Predicted
1	−10	30	400	8	69.35	72.26
2	−8	40	350	10	37.73	34.34
3	−12	40	350	10	86.76	87.39
4	−12	40	350	6	84.86	74.56
5	−12	40	350	14	55.54	63.43
6	−16	40	350	10	90.06	91.04
7	−10	50	400	12	46.02	50.31
8	−12	40	250	10	76.42	72.16
9	−10	50	400	8	46.09	45.29
10	−10	30	300	8	69.35	68.96
11	−14	30	400	8	84.14	86.77
12	−10	50	300	8	36.76	48.71
13	−14	50	400	8	72.86	76.55
14	−14	30	400	12	89.47	84.60
15	−12	20	350	10	76.94	79.28
16	−12	40	350	10	88.02	87.39
17	−10	30	300	12	45.49	48.89
18	−10	50	300	12	47.08	39.75
19	−12	60	350	10	64.66	59.92
20	−12	40	450	10	77.16	79.01
21	−14	50	400	12	89.81	85.49
22	−14	30	300	8	87.69	90.48
23	−14	50	300	12	77.76	81.94
24	−10	30	400	12	71.06	66.17
25	−14	50	300	8	86.80	86.98
26	−14	30	300	12	78.23	74.33

matrix was used to create the table for the chosen range of parameters. The software recommended 26 runs at five levels with two repetitions and an axial point; experiments were conducted based on this table to enable the PFC system to be optimised. After the optimization, the accuracy of the suggested model by RSM was validated by performing experiments on optimized conditions.

3. Results and discussion

3.1. Ice formation

At the end of each designated operation time in the experiments, it can be seen that an ice layer had been formed on the cooled probes of the MPCC as shown in Fig. 1(d). The lysozyme content was determined using the lysozyme solution standard graph calibrated using UV–vis

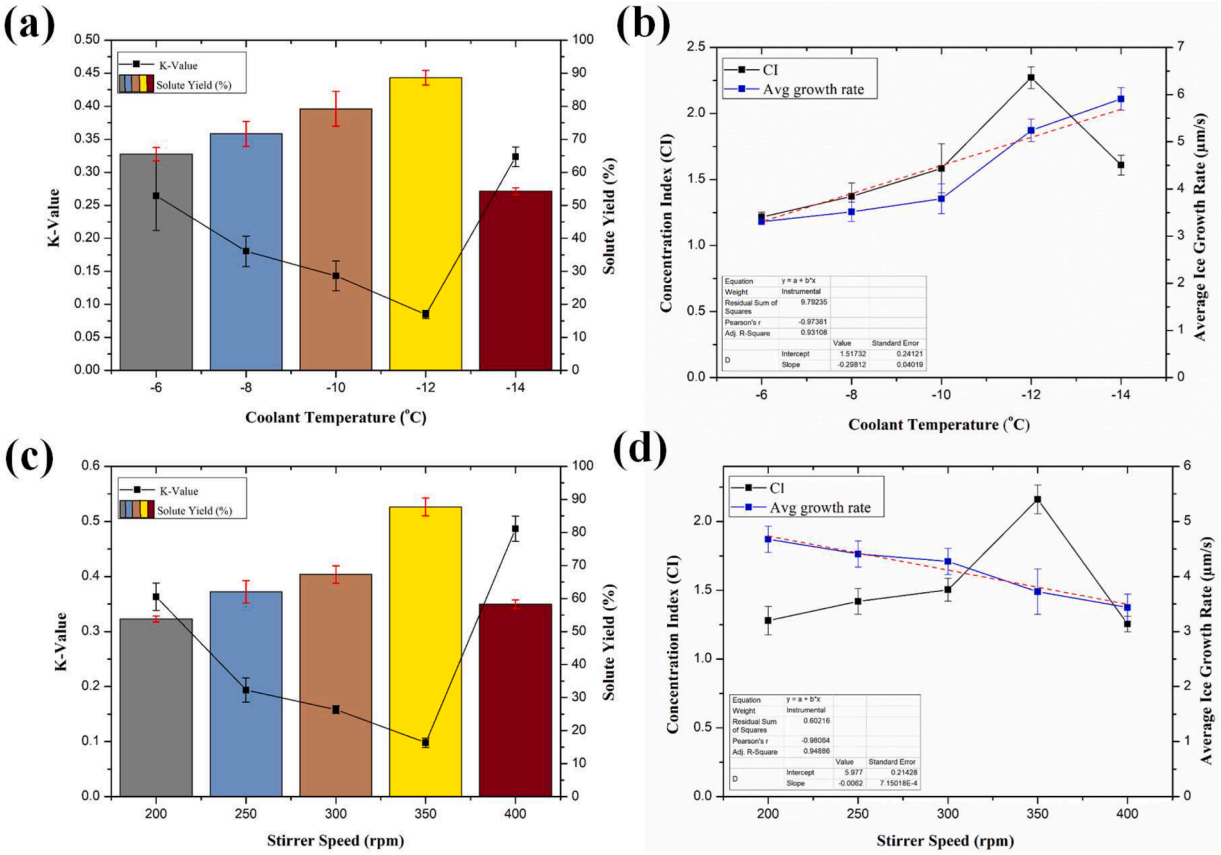

Fig. 3. Effect of different operating parameters; (a) Effect of coolant temperature on effective partition constant and solute yield, (b) Concentration index and average ice growth rate, (c) Effect of stirrer speed on K-value and solute yield and (d) Concentration index and average ice growth rate.

spectrophotometer [15]. The highest peak for lysozyme solution absorbance was observed at 280 nm using UV–vis spectrophotometer. In comparison, the concentrated lysozyme sample was seen to be thicker, portraying a higher concentration. Thawed ice was observed to be comparatively clearer than the initial lysozyme solution. The lysozyme concentration in the thawed ice and the residual solution was affected by the experimental settings, which included a coolant temperature of −10 to −14 °C, a stirrer speed of 200 to 400 rpm, an operation period of 20 to 60 min, and an initial lysozyme concentration of 6 to 14 mg/mL. The solute movement throughout the operation and thawing might have caused the migration of solutes to the liquid phase from the ice crystals, which leads to a clearer ice crystal and less concentrated solution [12].

3.2. Study of various operating parameters

3.2.1. Effect of coolant temperature

The behavioural study as affected by coolant temperature also served as an initial screening to select the range for the optimization study to be performed. Fig. 3(a) depicts the ratio of solute in the solid and liquid phase (K-value) and Y as the yield of the concentration achieved through MPCC system. Only until the temperature reached −6 °C during the experiment runs did the first layer of ice form, although it was still not solid. It was also observed that the ice layer filled the solution tank's space at −16 °C. Thus, for the optimization study, the coolant temperature range was decided accordingly between these two values, and determined to be from −10 to −14 °C, to provide some space for the extreme α values in the optimisation process. The coolant temperature is very important to control as it controls the solute loss from the solution [25]. The K-value was found to be lowest at a coolant temperature of −12 °C, while the solute concentration yield exhibited the highest values at this temperature, indicating the PFC system's efficiency through the MPCC process. Under these circumstances, it is advantageous that the solute concentration in the ice phase is lower than that in the liquid phase. Additionally, temperature has a direct proportionate effect on the rate of ice formation [25,26].

Although it is favourable to produce as much ice as possible to get the most concentrated solution. The setpoint for coolant temperature should be determined carefully as it could be higher than the solution's freezing temperature at the particular concentration. The setpoint for coolant temperature is significantly lesser than the pure water as it is affected by the freezing point depression phenomenon caused by the solute concentration [27]. In this investigation, lower coolant temperature resulted in a higher concentration of lysozyme in the liquid fraction, but not at the lowest (−14 °C). The lowest coolant temperature might have caused the ice growth to be too rapid, trapping the solute from its trajectory direction [28]. Fig. 3(a) clearly shows that, in tandem with an increase in solute concentration in the process' liquid phase, K-value falls when coolant temperature drops to −12 °C. However, K rose because of solute inclusion or the solute retained in the ice as a result of the rapid cooling at the lowest coolant temperature of −14 °C [29]. The high growth rate of ice crystals leads to the enhanced trapping of solutes between the ice dendrites that would transport heat away from the freezing front [30]. The solute yield in Fig. 3(a) is also derived from the mass solute ratio in the liquid fraction and beginning concentration. Similarly, the optimal coolant temperature was −12 °C, which yielded >90 % of the solute yield. Additionally, the K-value and solute yield are shown to be indirectly related to one another, with K-value decreasing as performance increases and Y increasing as the system performs at its peak. The lysozyme solution was more concentrated at lower coolant temperatures but slightly decreased at higher coolant temperatures, which is an interesting discovery.

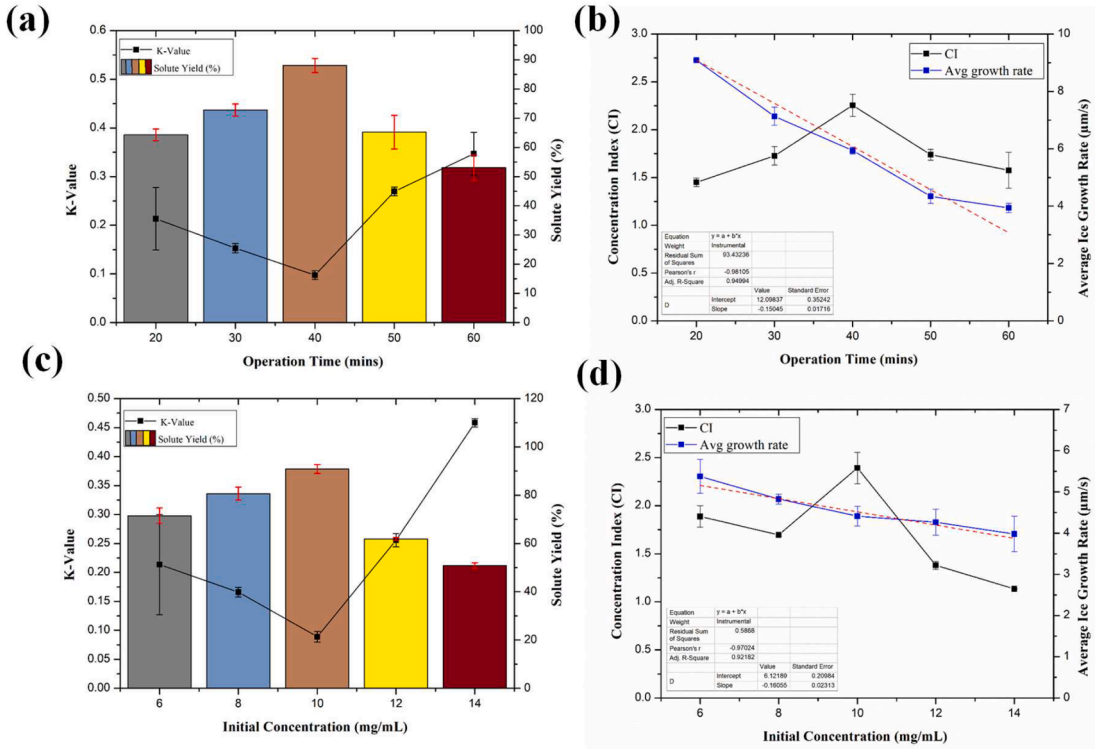

Fig. 4. Effect of different operating parameters; (a) Effect of operation time on effective partition constant and solute yield, (b) Concentration index and average ice growth rate, (c) Effect of initial concentration on K-value and solute yield and (d) Concentration index and average ice growth rate.

The eutectic mixture has an association with heat transfer and the ice-liquid interface, where the lysozyme aqueous solution requires a lower coolant temperature to allow pure water to form the crystal lattices [26]. The freeze concentration concept, which is established on the freezing and growing of ice crystals from aqueous solutions supports this phenomenon [3]. The ice crystal lattice would lead to the formation of a solution with enhanced concentration, which as a result will eliminate contaminants to accumulate pure crystal [31]. However, extremely low coolant temperatures will cause the solute's mass in the liquid solution to be trapped in the rapid growth of the ice at the lowest coolant temperature (−14 °C). To provide evidence on the ice growth that can be severely affected by the coolant temperature, a calculation of concentration index (CI) and average ice growth rate was performed giving out the plots in Fig. 3(b). It is observed from the figure that at the highest coolant temperature (i.e., −6 °C) concentration index (CI) was low and then it gradually increased with lower coolant temperatures applied afterwards. Theoretically, the solution inside the system should have first undergone a chilling process before continuing into freezing [26], this shows that the coolant temperature is insufficient to completely freeze the water present in the solution. The ice nuclei continued to develop into high-purity ice at other lower temperatures applied, giving the finest CI value at a coolant temperature of −12 °C because the temperature of the solution was low enough for nucleation to take place and subsequently grow to produce a solid block of ice crystal [12]. However, at −14 °C, the trend changed where the value of the CI decreased. At this lowest coolant temperature, the ice thickness was impressively the largest. However, a thicker ice layer does not necessarily indicate higher quality; not if the cooling process was done too rapidly which would induce higher solute entrapment in the solid matrix [26,32]. This is evident through the increased calculated ice growth rate at 5.91 μm/s at this temperature.

A higher value of ice growth rate was observed at low coolant temperatures [33]. The lower coolant temperature caused more dendritic ice to form, which can speed up the crystal formation by increasing the interface between the ice and the solution. According to Miyawaki et al. [34] the growing rate of ice crystals is controlled by the coolant temperature, whereas the creation of ice crystals is influenced by the cryo-concentration or freezing principle. The slow rate of ice growth can also be observed at the nucleation point where the solution temperature can be affected by the fusion heat released from the production of ice nuclei at the beginning of the ice crystallisation process these findings are in agreement with the previous literature [34]. However, because of a lower surface temperature and a larger temperature differential between the cold probe surface and the entering solution, the CI values at −14 °C, the coolant temperature, were slightly lower than at −12 °C. Additionally, it gave ice nucleation formation and appropriate initial supercooling, which has an impact on the enclosure of solute in the ice [25]. However, this phenomenon was found different for ice growth rate, as a direct relation was observed between the production of average ice growth rate and higher coolant temperature (−14 °C) that is 5.91 μm/s. Due to increased concentration at the solid-liquid interface solute loss increases and this phenomenon takes place [35].

3.2.2. *Effect of stirrer speed*

As the production and purity of ice crystal layer in PFC is greatly influenced by the solution movement which promotes the digression of solutes from the solid interface, the effect of stirrer speed was investigated. For screening, a stirrer speed of 100 rpm was first selected but unfortunately, it was observed that only a very thin layer of ice was formed due to the low interaction between solid-liquid or liquid-liquid interface and low heat transfer. The screening experiments were continued until the initial ice layer was formed on the probe's surface at the speed of 200 rpm. The stirrer speed of 400 rpm was selected based on the fact that the thickness of ice was reduced to the previous speed screened. The studies were conducted with a constant coolant temperature of −12 °C and in the 200–400 rpm range, based on the screening experiments. Furthermore, a 40 min operation period and a starting concentration of 10 mg/mL were chosen for additional testing. The findings from the screening process were also used to set the range for the RSM in the process optimisation afterwards. Fig. 3(c) illustrates at

200 rpm stirrer speed the K-value was found to be 0.36, which decreased to 0.098 when the stirrer speed was increased to 350 rpm. Furthermore, it was observed that the K-value was again increased to a value of 0.49 when the stirrer speed was increased to 400 rpm. This could be related to the phenomenon that took place due to a decrease in the driving force needed to remove the solute from the ice crystal layer and a tendency to accumulate more solute in the ice phase as compared to the liquid phase [36].

Additionally, at the applied constant coolant temperature heavy accumulation of solute was taking place at the ice-liquid interface, which led to increased solute concentration in the ice formed that requires swift washing provided by the stirrer speed to avoid poor separation as a result of the low purity of the ice produced [37,38]. Yahya et al. [32] claimed that high stirrer speed may lead to the favourable washing of ice that results in increased solute concentration in the liquid phase. However, extreme care for balance is needed because if the stirrer speed is too high, low ice volume might be yielded, hence making the production of highly concentrated lysozyme solution in the end impossible. It was observed that the solute yield of lysozyme in the liquid fraction was directly proportional to the stirrer speeds from 200 to 350 rpm. Theoretically, stirring a solution would give mass transfer and heat transfer dispersion to create ice crystals, but if the undercooling is occurring at a level within the metastable zone, crystallisation will not take place except that ice seeds are introduced into the solution [39]. This indicates that greater speed is required to create an ice crystal lattice on the probe's cold surface. During the crystallisation process, the heat transfer would also rise between the solution and the cooled surface, changing the distribution of kinetic energy under the impact of stirrer speed [40]. According to Ojeda et al. [41] agitation causes a positive movement in the liquid phase, resulting in a larger mass transfer coefficient that transfers the solid-liquid interface into the bulk of solution and affects concentration in the liquid phase. As a result, almost pure water would be produced upon separation from the formed ice layer.

However, when the stirrer was operating at a high speed of 400 rpm, less ice was formed, and the amount of water in the concentrate increased, lowering the concentration of the solution [39]. Fig. 3(d) depicts that the CI increased with an increase in stirrer speeds giving its maximum at 350 rpm, in contrast with the average ice growth rate which kept decreasing with the increased solution movement. Both CI and ice growth rates are not favourable at 400 rpm. The ice volume at 400 rpm might be low because of the shear force created by the solution movement from the rapid stirrer speed, thus producing a low average ice growth rate. As much as the high ice volume is needed for a good concentration efficiency, the entrapment of solutes in it has to be considered as well. Thus, although 200 rpm can produce the largest volume of ice, it was not in the cleanest state, resulting in a lower CI value than 350 rpm. Low fluid motion from low stirrer speeds influences the mass transfer rate from the ice front to the liquid fraction [29]. These findings correlate with the earlier studies where lower productivity was reported to be independent of concentration [42]. At reasonably high stirrer speeds, the high velocity makes the solutes redistribute themselves during the ice crystallization, and kinetic expansion of the ice front phenomenon also takes place which makes the solutes diffuse away from the ice solution interface into the bulk solution [40]. Although with reduced ice mass, enrichment of solute in the bulk solution made the CI increase because the ice layer still maintains its purity. Implementing different stirrer speeds allowed for the dispersion of mass and heat in the solution. As the heat was transferred to the cooling probe, this encouraged the ice crystal layer to form on the cooled probe wall [38].

3.2.3. Effect of operation time

The impact of operation time was studied by performing experiments for 20, 30, 40, 50 and 60 min. To perform this, other parameters such as coolant temperature (−12 °C), stirrer speed (350 rpm) and initial concentration (10 mg/mL) were kept constant. The changes in the mass fraction of lysozyme (solute yield) and the ratio of the lysozyme aqueous solution concentration in the liquid and ice phases (K-value) during the freeze concentration process are shown in Fig. 4(a). The experimental data showed that both responses had a varying tendency toward the operation time. The impurity of the ice grew with time and concentration, which caused the K-value and yield to be higher and lower, respectively. The first 20 min were insufficient for the freezing process to produce complete ice layer creation and were impacted by the ice fraction [38]. Due to the limited heat transfer interaction at the ice-liquid interface, this led to an unstable ice structure [29]. This situation would be regarded as an unstable state for the solid ice phase since it arises from an incomplete freezing process. The optimal K-value and solute yield, with 0.0928 and 88.04 %, respectively, were found at 40 min as compared to other operating times. The initial concentration evolved because, for the particular operating period used, the mass and heat transfer of the entire process was at equilibrium, which correlates to the solute inclusion constraints [41].

Flesland et al. [43] reported that solute diffusion into the bulk of solution from the ice-liquid interface is required to balance the steady state of ice formation on the probe's cold surface and the proportion of solute. Consequently, when crystallised ice first forms and begins to develop, the solute is rejected by the ice crystal lattice because of its large molecule size, and the impurities are expelled to create a pure ice crystal lattice [44,45]. Nevertheless, the K-value increased and the solute yield decreased after 40 min. This demonstrates that a longer operation time also offsets the rise in solute enclosure in ice and contributes to the alteration of values for both responses. The solute yield was smaller at 50 min and lower at 60 min (65.22 % and 53.06 % respectively) while K-value increased. Although solute was lost more and more in the ice phase as the operation time increased beyond 40 min, the mass of solutes collected in the liquid was still higher than the solid fraction along with the operation time [46].

From Fig. 4(b) it was observed that CI increased with respect to operation time until 40 min, but then declined beyond that value. This could be attributed to the unsteady state of ice nucleation and mass transfer of the process at the initial stage of freezing giving a lower concentration ratio in contrast to the liquid phase's concentration [21]. The heat from the crystallisation process is released into the environment or upon the cold surface of the probe during freezing when the ice crystal lattice starts developing. This heat then tends to elute the solute, producing a pure ice crystal layer [47]. As a result, the process would eliminate the contaminants, leaving the solutes in the bulk solution [31]. As time proceeded, a higher amount of solute remaining in the liquid could result in solute concentration occupying the space in the dendritic ice to increase, lowering the CI [48]. The figure also shows that $\tilde{v}_{ice}$ was higher at the start which decreased over time. This may be because of the reason that heat transfer resistance and interface from the solution concentration increase over time [21]. The higher concentration of solutes in the liquid fraction also made freezing more challenging by lowering the solution's freezing point. The lower $\tilde{v}_{ice}$ should favour the FC process but an opposite phenomenon was observed. The CI decreased with the lower $\tilde{v}_{ice}$ because as anticipated, longer operation time would yield thicker ice, leaving only a small path for solute trajectory which would cause them to migrate into the ice layer. More solute will be entrained in the ice as a result, further thickening the ice [40].

3.2.4. Effect of initial concentration

The last variable, starting concentration, is anticipated to affect the solution's freezing point because of the number and kinds of solutes present. As is well known, the freezing point of a solution will change if the solute's molecular weight (MW) is low. This is because of the reason that as molar mass increases, the depression of the freezing point decreases. This implies that a solution's lower freezing point will result from a larger initial concentration of the solution [41]. As a result of the screening process, the initial concentration was studied between 6, 8, 10, 12 and 14 mg/mL. In addition, the coolant temperature (−12 °C), the

Table 5
Regression coefficients and ANOVA of second-order polynomial model for effective partition constant and solute concentration yield.

Source	Mean square		Df	F-Ratio		P-Value	
	K-value	Yield (%)		K-value	Yield (%)	K-value	Yield (%)
X_1:	0.1685	4822.90	1	83.52	89.29	0	0
X_2:	0.0036	562.214	1	1.820	10.41	0.2042	0.0081
X_3:	0.0195	70.4523	1	9.690	1.300	0.0099	0.2777
X_4	0.0059	185.704	1	2.940	3.440	0.1147	0.0907
X_1^2	0.0704	665.238	1	34.94	12.32	0.0001	0.0049
X_2^2	0.0035	345.223	1	4.260	6.390	0.0633	0.0281
X_3^2	0.0329	151.877	1	4.310	2.810	0.0621	0.1217
X_4^2	0.0100	368.903	1	4.960	6.830	0.0477	0.0241
$X_1 \times_2$	0.0003	280.562	1	0.170	5.190	0.6923	0.0436
$X_1 \times_3$	0.0011	49.1401	1	0.580	0.910	0.4618	0.3607
$X_1 \times_4$	0.0086	15.3664	1	4.260	0.280	0.0433	0.6044
$X_2 \times_3$	0.0036	45.1584	1	1.800	0.840	0.2068	0.3801
$X_2 \times_4$	0.0086	123.432	1	4.310	2.290	0.0421	0.1588
$X_3 \times_4$	0.0009	195.720	1	16.32	3.620	0.0020	0.0835
Total error	0.0020	54.0164	11				
Total (corr.)			25				

Table 6
Error predictions from generated models for effective partition constant and solute concentration yield.

Error prediction	K-value	Yield (%)
R^2	0.9444000	0.92304
MAE	0.0225737	3.82843
SEE	0.0449177	7.34958
CV (%)	5.45	6.83

Note: R^2= Regression coefficient, MAE= Mean Absolute Error, SEE= Standard Error of Estimation and CV= Coefficient of variance.

stirrer speed (350 rpm), and the operating time were all kept constant (40 min). The data was analysed using Fig. 4(c) shows that the increase in initial concentration inversely effects the K-value and solute yield. This demonstrates that, for all constant stirring speeds, a lower initial concentration provides a higher product concentration [12].

At a lower initial concentration (i.e., 6 mg/mL) high purity ice was produced which gives a low K-value. It is clear from Fig. 4(c) that an initial concentration of 10 mg/mL showed the best results for K-value (0.089) as well as for solute yield (90.85 %). Due to larger solutes of lysozyme elimination or remaining in the concentrated liquid as ice dendritic filaments create a stable structure and would escape inclusion in the ice [37]. Additionally, it was discovered that the K-value abruptly increased to a higher value, from 0.089 to 0.46 whereas solute yield decreased gradually from 90.85 % down to 50.85 % when the experiments were performed at a higher initial concentration. This could be explained by the fact that more solute occlusion would happen in the ice at a high starting concentration [49]. As a result of this gradual reduction in solute yield, the freezing point dropped and the heat transfer resistance as well as ice thickness was increased. As indicated by Miyawaki et al. [34], the initial concentration significantly influences the mass transfer rate of the solute in the ice. From Fig. 4(c) it is evident at a higher initial concentration ((i.e., 14 mg/mL) solute yield dropped noticeably. Because of the increased initial concentration, the solution had a high viscosity but a low diffusivity coefficient, this may lead to a higher growth rate of secondary ice nucleation known as dendritic formation to entrap the solute [31]. The best CI was obtained at an initial dosage of 10 mg/mL, as shown in Fig. 4(d), while the trend slightly altered when the starting concentration was maintained at lower values. Theoretically, slow ice growth would prevent contaminants from becoming congested, and the ice's crystal structure is sufficient to reduce the quantity of solute trapped in the ice surface [48,50].

Additionally, the potential for achieving large concentrations is increased by the achievement of solid-liquid equilibrium of solution concentration where water is used as a solvent. Although there is a completely different relationship between CI and ice growth rate at lower initial concentrations. It was observed that the result gradually changed to the same trend at higher initial concentrations, especially for initial concentrations of 12 mg/mL and 14 mg/mL because of the increased solute saturation and solid obstruction in the ice [29]. A linear line of ice reduces with increasing initial concentration during the freezing process, as seen in Fig. 4(d). This is caused by the heat resistance generated during the process of freezing an ice layer [50]. In addition, raising the solution concentration would make the solution more viscous, which would lower the solute diffusivity [41].

3.3. Statistical analysis and optimization

The following polynomial expression (Eq. (7)) was produced to associate the K-value and solute yield with other independent variables. Where X are the experimental variable that influences the process. Through Analysis of variance (ANOVA) the value of R^2 for the regression model in this MPCC design was calculated to be 94.444 % and 92.304 % for K-Value and solute concentration Yield (%) respectively using Eq. (7) and Eq. (8) respectively. According to Rashid et al. [23] R^2 values in the range of 88–90 % are considered to be significant for the model validation. Hence, 94.44 % and 92.30 % are considered quite moderate to validate the fit. When describing the validity of the created model, the response value of R2 is thought to be good. The more closely the empirical model matches the actual data, the closer the R2 value is to unity [51]. The statistical analysis of data (analysis of variance) ANOVA depicts ≈ 92 % reliability of K-value and solute yield. The adequacy of the quadratic model generated was checked based on a probability p-value of <0.05 (i.e., 95 % confidence level) and a higher F-value [51].

$$\begin{aligned}\text{Kvalue} = {} & 3.04138 + 0.376542\times X_1 + 0.00935833\times X_2 - 0.00972917\times X_3 + 0.131562\times X_4 + 0.015888\times X_1{}^2 \\ & - 0.000228125\times X_1X_2 + 0.000085625\times X_1X_3 - 0.00579688\times X_1X_4 + 0.000141771\times X_2{}^2 - 0.000030125\times X_2X_3 \\ & - 0.00116563\times X_2X_4 + 0.0000173708\times X_3{}^2 - 0.000076875\times X_3X_4 - 0.00598698\times X_4{}^2\end{aligned} \tag{7}$$

$$\begin{aligned}\text{Soluteyield}(\%) = {} & -342.049 - 39.4379\times X_1 + 0.348583\times X_2 + 0.855158\times X_3 + 0.859375\times X_4 - 1.54339\times X_1{}^2 - 0.209375\times X_1X_2 + 0.017525\times X_1X_3 \\ & 0.245\times X_1X_4 - 0.0444729\times X_2{}^2 - 0.00336\times X_2X_3 + 0.138875\times X_2X_4 - 0.00117992\times X_3{}^2 + 0.034975\times X_3X_4 - 1.14932\times X_4{}^2\end{aligned} \tag{8}$$

3.4. Validation of response surface model

The regression modelling results obtained from CCD experiments are tabulated in Table 5. Each model showed high significance with a low p-value (<0.0001) and high F-value [51]. This implies that the models generated are significant. Table 6 shows that these models are statistically acceptable as the values for the coefficient of variance (CV %) are <10 % [23,52]. Table 5 demonstrates that the quadratic terms of coolant temperature (X12), initial concentration (X42), and stirrer speed (X3)

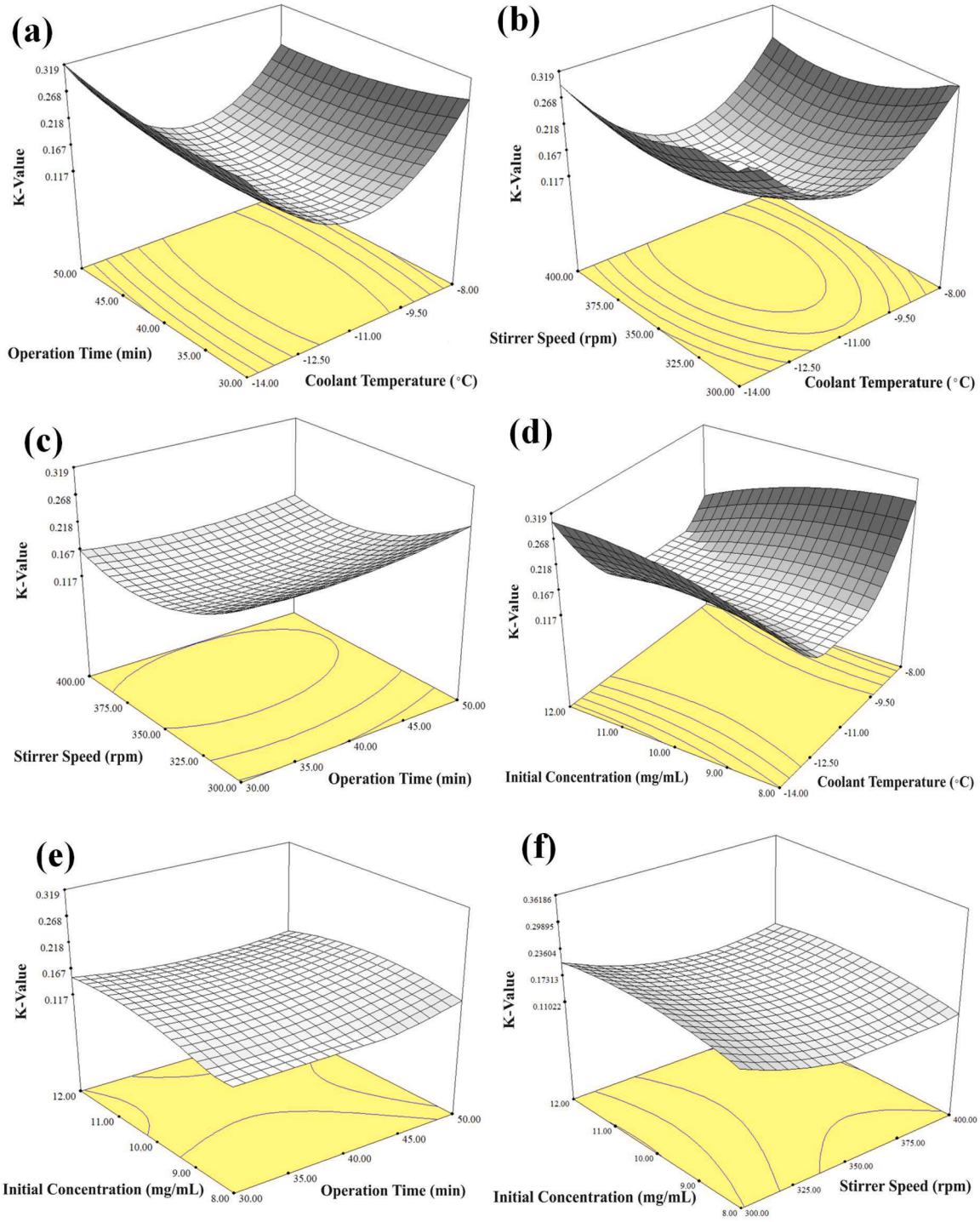

Fig. 5. Response surface plots for interaction effects of variables on effective partition constant; (a) Interaction effect of operation time and coolant temperature, (b) Interaction effect of stirrer speed and coolant temperature, (c) Interaction effect of stirrer speed and operation time, (d) Interaction effect of initial concentration and coolant temperature, (e) Interaction effect of initial concentration and operation time and (f) Interaction effect of initial concentration and stirrer speed.

are significant (i.e., $p < 0.05$) for K-value. Conversely, for the K-value (i.e., $p < 0.05$), it was also discovered that the interaction effects of stirrer speed and initial concentration (X3×4), operating duration and initial concentration (X2×4), and coolant temperature and initial concentration (X1×4) were significant. The linear term of operation time (X2) and the quadratic terms of coolant temperature (X12), operation time (X22), and beginning concentration (X42) for solute concentration yield (%) may be found to have a significant response (i.e., $p < 0.05$). Moreover, the interaction effects of coolant temperature and operation time ($X_1 \times_2$) were found significant for the solute concentration yield. The 3D response surface plots in the following section provide a detailed explanation of the factors that interact between independent variables and responses.

3.5. Response surface plot analysis

For the best possible visualisation of each response variable, 3D plots were plotted, while varying one variable and holding the other two

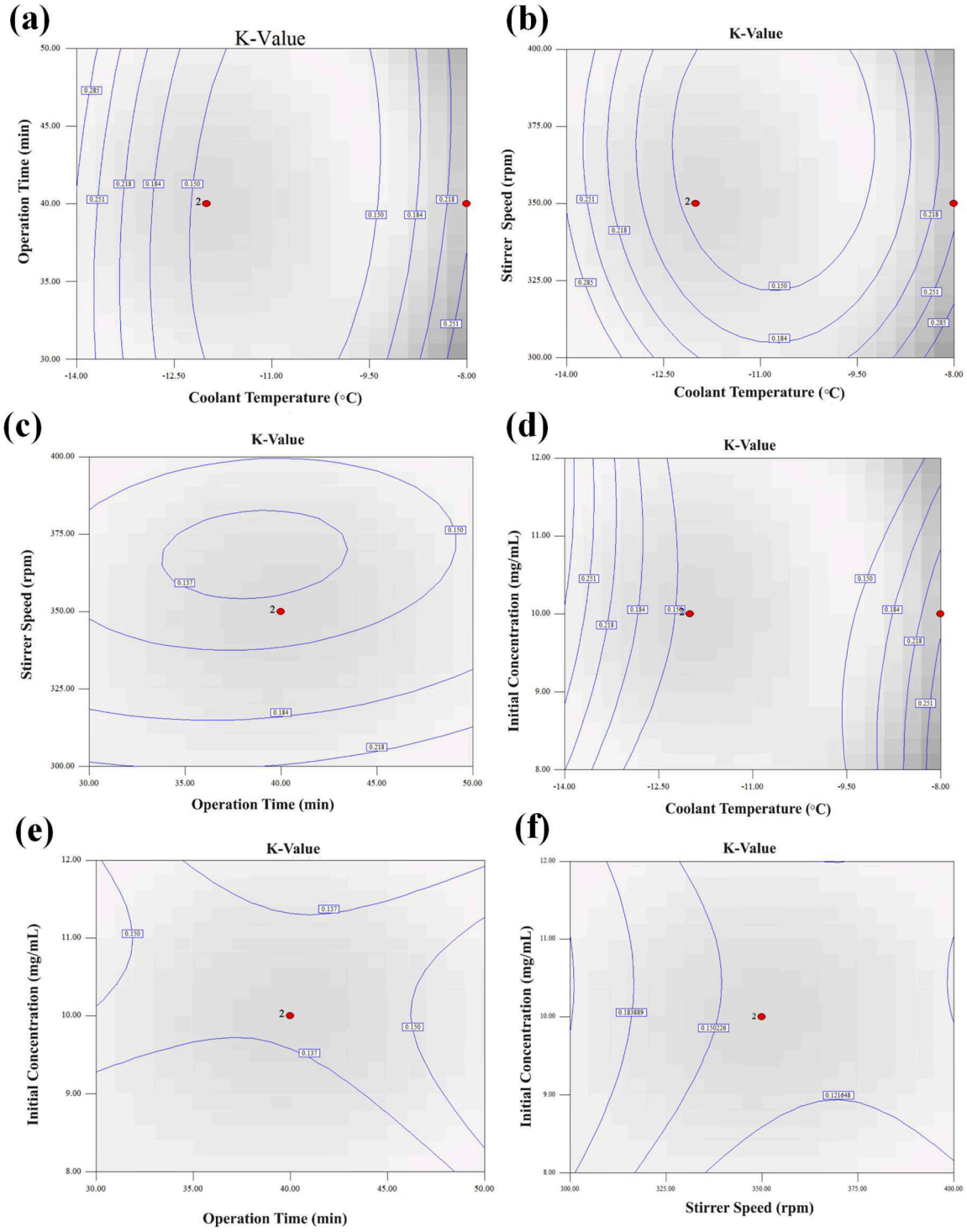

Fig. 6. 2D contour plots for interactions between different variables on effective partition constant; (a) Operation time and coolant temperature, (b) Stirrer speed and coolant temperature, (c) Stirrer speed and operation time, (d) Initial concentration and coolant temperature, (e) Initial concentration and operation time and (f) Initial concentration and stirrer speed.

variables as constant, these interpretations were produced against two variables to investigate the consequences of their interactions. Afterwards, it was determined and discussed how the two independent variables related to each other.

3.5.1. Interaction of variables on effective partition constant

The factors that significantly affect the process were identified after validating and assessing the regression model's significance. The calculated multiple regression findings are exhibited in Table 5, which also includes a list of all significant and insignificant values for each factor and their interactions. The 3D plots (Fig. 5(a) and (b)) depict the interaction effects of coolant temperature with operation time, and stirrer speed as well as the combined effect of operation time and stirrer speed (Fig. 5(c)) are significant. The contour plots (Fig. 6(a) to (c)) clearly show that the small circular area contains the maximum predicted value. The contour plots having elliptical or circular shapes

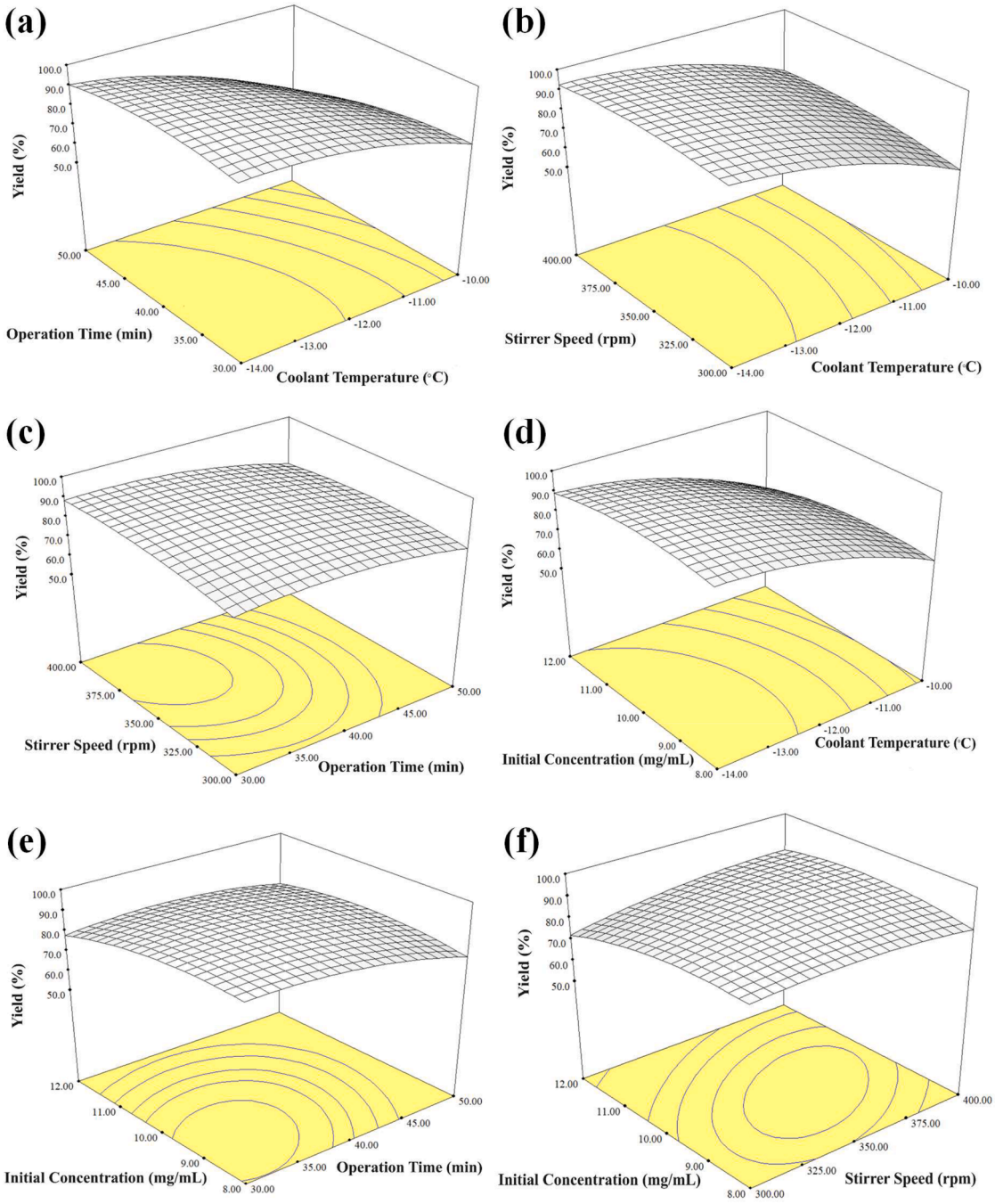

Fig. 7. Response surface plots for interaction effects of different variables on solute concentration yield; (a) Operation time and coolant temperature, (b) Stirrer speed and coolant temperature, (c) Stirrer speed and operation time (d) Initial concentration and coolant temperature, (e) Initial concentration and operation time and (f) Initial concentration and stirrer speed.

represent how relevant the variables are [23,53]. The elliptical contour plots indicate the importance of the variables and the impact of their interactions. It is clear from Fig. 5(a) and (b) that operation time (35 min) and stirrer speed (400 rpm) have a significant effect on K-value, hence increasing both of the factors can improve the effectiveness of the concentration process. The interaction impact between coolant temperature and stirrer speed is likewise considerable with respect to K-value as shown in Fig. 5(b). At increased stirrer speeds and coolant temperatures between −9 and −12 °C, the K-value decreased. A higher K-value denotes a worse PFC system efficiency; it was found that the K-value sharply rose when the applied coolant temperature exceeded the range, or −14 °C.

The 3D plots present that at stirrer speed > 400 rpm, operation time ≤ 35 min, consistent temperature of −12 °C and an initial concentration of 10 mg/mL lower K-values were observed.

Showing that a higher stirrer speed and lower initial concentration of solution results in a reduced K-value (Fig. 5(f)). These results are in alignment with the findings of Zhang et al. [54] stating that coolant temperature is the controlling factor in the rate of ice formation. When a coolant temperature is provided that is too low, the solute is easily trapped, hence increasing the K-value. As seen in Fig. 5(a), a larger growth rate at the lowest coolant temperature may result in a lower K-value, hence increasing the ice purity. In contrast, the interaction effects of operation time and initial concentration Fig. 5(e) showed that

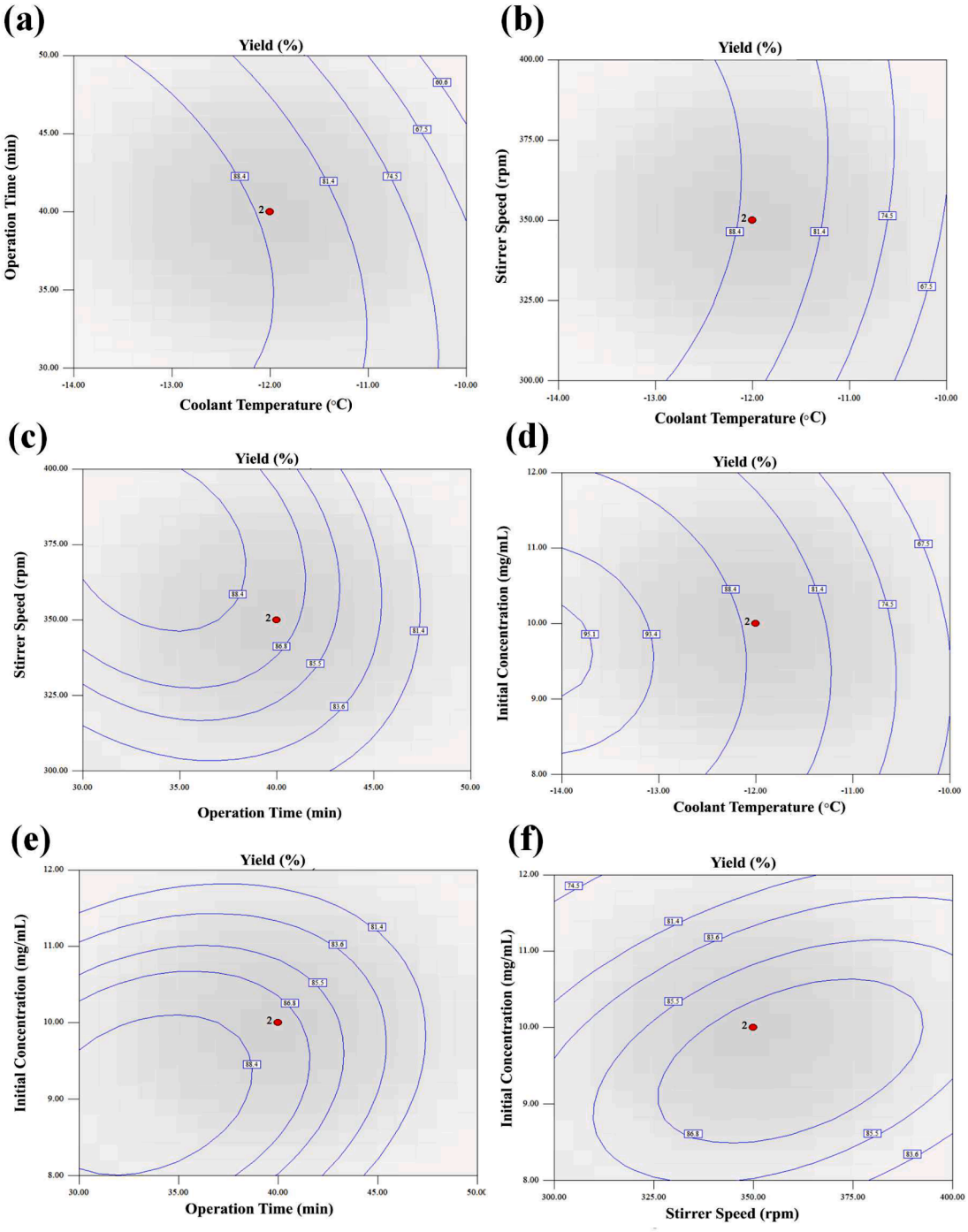

Fig. 8. 2D contour plots for interactions between different variables on solute concentration yield; (a) Operation time and coolant temperature, (b) Stirrer speed and coolant temperature, (c) Stirrer speed and operation time, (d) Initial concentration and coolant temperature, (e) Initial concentration and operation time and (f) Initial concentration and stirrer speed.

larger operation times and lesser initial concentrations lead to lower K-values, demonstrating that the PFC system can operate at high efficiency under these conditions. These results are in alignment with the findings of [48] stating that a greater operation time required for ice formation on the probe's cold surface is because of the depression in the freezing point and phenomenon of supercooling. In addition, Table 5 shows that some of the coefficients are insignificant (i.e., $p > 0.05$), the insignificance of these coefficients and their impacts cannot be ignored to defend the model's overall standing [23].

3.5.2. *Interaction of variables on solute concentration yield*

The purity of the ice crystal in the PFC process is embodied by the solute concentration yield. The efficiency of this PFC system is best described by high solute concentration yield. The interaction effects between each variable level and solute concentration yield are shown in Figs. 7 and 8. From ANOVA (Table 5), although in terms of a single effect initial concentration is not significant, its quadratic effects seem significant. As seen in Fig. 7(d), low initial concentrations (i.e., <10 mg/mL) and coolant temperatures between −10 to −12 °C can result in an acceptable development of ice crystals. Meanwhile, it is evident from Fig. 7(f) that the maximum stirrer speed and lowest initial concentration

Table 7
Predicted optimal conditions for the model's validation.

	Optimum operating conditions			Predicted values	
Coolant temperature	Operation time	Stirrer speed	Initial concentration		
X_1 (°C)	X_2 (min)	X_3 (rpm)	X_4 (mg/mL)		
−12.69	34.50	387	10.00	K-value	0.132
−11.85	33.49	389	10.43	Yield (%)	87.39

are the conditions that lead to the greatest solute concentration yield. This is because the high liquid flow rate and high shear force could remove the solute from the solution without allowing it to become trapped in the ice layer that is being developed. Likewise, the solutes confined in the dendritic ice structure may simply be removed by the shear force [32]. It can be concluded that the major factors influencing the PFC process are freezing points and solution viscosity [55].

The optimal combination of variables i.e., initial concentrations<10 mg/mL and operating times > 35 min were observed, as illustrated in Fig. 7(e), which also depicts the interaction between factors (initial concentration and operation time) on solute concentration yield. John et al. [44] reported that the efficiency of PFC decreases with an enhanced initial concentration due to the solute contents which are trapped in the ice crystal layer. Briefly, solute concentration yield starts to decline and eventually becomes essentially static as the initial concentration exceeds 10 mg/mL, indicating reduced system efficiency. The interaction impact of starting concentration with stirrer speed and operating time is clearly seen in Fig. 7(c) and (e) (circular contours). It was discovered that stirrer speed values between 380 rpm and − were ideal. However, erosion could lead to a less concentrated solution if the stirrer speed is applied too high. This is because the ice crystal's capacity to transfer heat is improved when the solutes are kept out of the ice-liquid interface [48]. As a result, the ice layer created contains less solute. In general, optimal conditions i.e., longer operation times result in thicker ice formation, but faster stirrer speeds produce solid ice with a high purity level. It might eventually wash the solutes from the dendritic ice formation away [25,44].

3.6. Model validation and optimum conditions

The R^2 for K-value and solute concentration yield indicates up to 94.44 % and 92.304 % variability of the response (Table 6) respectively. The impacts of factors like coolant temperature, operating time, stirrer speed, and beginning concentration are adequately described by the 3D response surface plots. Improved mass and heat transfers could be the outcome of the ideal combination of variables and an increased ice crystallisation surface area between the coolant and the lysozyme solution [28]. Which could be used to explicitly describe the interaction phenomena between variables. For the identification of the ideal and anticipated values, the optimized set of conditions is displayed in Table 6. Experiments were performed on these optimized conditions and the experimental results were in alignment with the model predicted values (Table 7). Table 7 depicts that the results of optimization of lysosome concentration are in alignment with the whey protein concentration optimized results [8]. The response surface model (Eq. (7) and Eq. (8)) created for the K-value and solute concentration yield showed an overall standard error of estimation of 0.044 and 7.349, respectively, as shown in Table 6 This demonstrates the current model's suitability and correctness.

4. Conclusion

This work has successfully investigated how the designed MPCC can work to concentrate lysozyme aqueous solution as desired for the food and pharmaceutical industry to make various products from it. The design of the apparatus has a comparatively higher surface area for heterogeneous ice nucleation and crystallization (87.39 or 35.44 % higher) compared with the conventional PFC system, which can improve the system's efficiency. Regression models based on CCD by RSM were used to optimise solute yield and K-value in addition to observing the effects of each operating parameter. Multi-response optimisation was used to assess multiple replies successfully, which is important to take into account at large production scales. The models were validated under the optimal circumstances, which were −11.85 °C, 33.49 min, 389 rpm, and 10.43 mg/mL for solute concentration yield and −12.69 °C, 34.50 min, 387 rpm, and 10 mg/mL for K-value, respectively. On the chosen optimised settings, the experimental findings were found to be in agreement with the model-predicted values of K-value 0.132 and solute concentration yield 87.39 %. This research may result in lower costs and energy consumption as well as the provision of several effective techniques for cold solute separation that also improve product quality and yield. The study's conclusions may help researchers scale up their investigation in order to commercialise this innovative lysozyme concentration technique that replaces traditional thermal processing with an improved and unique non-thermal processing design.

CRediT authorship contribution statement

Tazien Rashid: Writing – original draft, Resources, Conceptualization. **Mazura Jusoh:** Writing – review & editing, Supervision, Resources, Funding acquisition, Conceptualization. **Zaki Yamani Zakaria:** Writing – original draft, Methodology, Formal analysis. **Norshafika Yahya:** Writing – review & editing, Validation, Formal analysis. **Sabah Ansar:** Writing – review & editing, Funding acquisition. **Tiong Sieh Kiong:** Writing – review & editing, Visualization, Software. **Farooq Sher:** Writing – review & editing, Project administration, Funding acquisition.

Declaration of competing interest

The authors declare that they have no known competing financial interests or personal relationships that could have appeared to influence the work reported in this paper.

Data availability

Data will be made available on request.

Acknowledgement

The authors are grateful to the Universiti Teknologi Malaysia and the Ministry of Education Malaysia (MOE) for their financial support through the Research University Grant and Fundamental Research Grant Scheme under the Vot no 04H46 and 4F224 respectively. The authors are grateful to the Researchers Supporting Project number (RSP2024R169), King Saud University, Riyadh, Saudi Arabia, for the financial support. The authors are also thankful for the financial support from the International Society of Engineering Science and Technology (ISEST) UK

References

[1] N. Khorshidian, E. Khanniri, M.R. Koushki, S. Sohrabvandi, M. Yousefi, An overview of antimicrobial activity of lysozyme and its functionality in cheese, Front. Nutr. 9 (2022) 833618.

[2] Jusoh, M., N. Ngadi, A. Johari, and Z.Y. Zakaria. Prediction of crystal mass through heat transfer study for a progressive freeze concentration system. 2014.

[3] M. Osorio, F.L. Moreno, M. Raventós, E. Hernández, Y. Ruiz, Progressive stirred freeze-concentration of ethanol-water solutions, J. Food Eng. 224 (2018) 71–79.

[4] A. Najim, S. Krishnan, A similarity solution for heat transfer analysis during progressive freeze-concentration based desalination, International Journal of Thermal Sciences 172 (2022) 107328.

[5] I. Seifert, W. Friess, Freeze concentration during freezing: how does the maximally freeze concentrated solution influence protein stability? Int. J. Pharm. 589 (2020) 119810.

[6] U. Roessl, S. Leitgeb, B. Nidetzky, Protein freeze concentration and micro-segregation analysed in a temperature-controlled freeze container, Biotechnology Reports 6 (2015) 108–111.

[7] Rosli, N.N.H.M., N.H. Harun, R.A. Rahman, N. Ngadi, S. Samsuri, N.A. Amran, N.Z. Safiei, F.H. Ab Hamid, Z.Y. Zakaria, and M.J.J.o.C.P. Jusoh, Preservation of total phenolic content (TPC) in cucumber juice concentrate using non-thermal Progressive Freeze Concentration: quantitative design characteristics and process optimization. 2022. 330: p. 129705.

[8] L.E.N. Ekpeni, K.Y. Benyounis, J. Stokes, A.G. Olabi, Improving and optimizing protein concentration yield from homogenized baker's yeast at different ratios of buffer solution, Int. J. Hydrogen. Energy 41 (37) (2016) 16415–16427.

[9] N. Szerman, C.B. Gonzalez, A.M. Sancho, G. Grigioni, F. Carduza, S.R. Vaudagna, Optimization of whey protein concentrate and sodium chloride concentrations and cooking temperature of sous vide cooked whole-muscle beef from Argentina, Meat Sci. 79 (3) (2008) 557–567.

[10] D. Parés, M. Toldrà, E. Camps, J. Geli, E. Saguer, C. Carretero, RSM Optimization for the Recovery of Technofunctional Protein Extracts from Porcine Hearts, Foods. 9 (12) (2020).

[11] S.K. Bermingham, A.M. Neumann, H.J. Kramer, P.J. Verheijen, G.M. van Rosmalen, J. Grievink, A design procedure and predictive models for solution crystallisation processes, in: AIChE Symposium Series. 2000, American Institute of Chemical Engineers, New York, 1998.

[12] N.N.H. Mohd Rosli, N.H. Harun, R. Abdul Rahman, N. Ngadi, S. Samsuri, N. A. Amran, N.Z. Safiei, F.H. Ab Hamid, Z.Y. Zakaria, M. Jusoh, Preservation of total phenolic content (TPC) in cucumber juice concentrate using non-thermal Progressive Freeze Concentration: quantitative design characteristics and process optimization, J. Clean. Prod. 330 (2022) 129705.

[13] T. Santana, J. Moreno, G. Petzold, R. Santana, G. Sáez-Trautmann, Evaluation of the Temperature and Time in Centrifugation-Assisted Freeze Concentration, Applied Sciences 10 (24) (2020) 9130.

[14] Y. Wang, A. Lomakin, R.F. Latypov, J.P. Laubach, T. Hideshima, P.G. Richardson, N.C. Munshi, K.C. Anderson, G.B. Benedek, Phase transitions in human IgG solutions, J. Chem. Phys. 139 (12) (2013) 121904.

[15] J.E. Noble, Quantification of protein concentration using UV absorbance and Coomassie dyes, Methods Enzymol. 536 (2014) 17–26.

[16] O. Miyawaki, C. Omote, M. Gunathilake, K. Ishisaki, S. Miwa, A. Tagami, S. Kitano, Integrated system of progressive freeze-concentration combined with partial ice-melting for yield improvement, J. Food Eng. 184 (2016) 38–43.

[17] O. Miyawaki, L. Liu, K. Nakamura, Effective Partition Constant of Solute between Ice and Liquid Phases in Progressive Freeze-Concentration, J. Food Sci. 63 (5) (1998) 756–758.

[18] G. Petzold, J.M. Aguilera, Centrifugal freeze concentration, Innovative Food Sci. Emerging Technol. 20 (2013) 253–258.

[19] A.A. Prestes, C.V. Helm, E.A. Esmerino, R. Silva, A.G. da Cruz, E.S. Prudencio, Freeze concentration techniques as alternative methods to thermal processing in dairy manufacturing: a review, J. Food Sci. 87 (2) (2022) 488–502.

[20] I. Uald-lamkaddam, A. Dadrasnia, L. Llenas, S. Ponsá, J. Colón, E. Vega, M. Mora, Application of Freeze Concentration Technologies to Valorize Nutrient-Rich Effluents Generated from the Anaerobic Digestion of Agro-Industrial Wastes, Sustainability. 13 (24) (2021) 13769.

[21] P. Chen, X.D. Chen, K.W. Free, Solute inclusion in ice formed from sucrose solutions on a sub-cooled surface—An experimental study, J. Food Eng. 38 (1) (1998) 1–13.

[22] P. Chen, X.D. Chen, A generalized correlation of solute inclusion in ice formed from aqueous solutions and food liquids on sub-cooled surface, Can. J. Chem. Eng. 78 (2) (2000) 312–319.

[23] T. Rashid, S. Ali Ammar Taqvi, F. Sher, S. Rubab, M. Thanabalan, M. Bilal, B. ul Islam, Enhanced lignin extraction and optimisation from oil palm biomass using neural network modelling, Fuel 293 (2021) 120485.

[24] H. Hassan, S.K. Adam, E. Alias, M.M.R. Meor Mohd Affandi, A.F. Shamsuddin, R. Basir, Central Composite Design for Formulation and Optimization of Solid Lipid Nanoparticles to Enhance Oral Bioavailability of Acyclovir, Molecules. (18) (2021) 26.

[25] S. Moharramzadeh, S.K. Ong, J. Alleman, K.S. Cetin, Parametric study of the progressive freeze concentration for desalination, Desalination. 510 (2021) 115077.

[26] S. Samsuri, N.A. Amran, M. Jusoh, Modelling of heat transfer for progressive freeze concentration process by spiral finned crystallizer, Chin. J. Chem. Eng. 26 (5) (2018) 970–975.

[27] J.E. Curtis, A. McAuley, H. Nanda, S. Krueger, Protein structure and interactions in the solid state studied by small-angle neutron scattering, Faraday Discuss. 158 (0) (2012) 285–299.

[28] S. Samsuri, N. Amran, M. Jusoh, Optimization of progressive freeze concentration on apple juice via response surface methodology, in: IOP Conference Series: Materials Science and Engineering, IOP Publishing, 2018.

[29] F.L. Moreno, M. Raventós, E. Hernández, Y. Ruiz, Behaviour of falling-film freeze concentration of coffee extract, J. Food Eng. 141 (2014) 20–26.

[30] Y. Yang, Y. Lu, J. Guo, X. Zhang, Application of freeze concentration for fluoride removal from water solution, J. Water. Process. Eng. 19 (2017) 260–266.

[31] K. Nakagawa, S. Maebashi, K. Maeda, Freeze-thawing as a path to concentrate aqueous solution, Sep. Purif. Technol. 73 (3) (2010) 403–408.

[32] N. Yahya, N. Ismail, Z.Y. Zakaria, N. Ngadi, R.A. Rahman, M. Jusoh, The Effect of Coolant Temperature and Stirrer Speed for Concentration of Sugarcane via Progressive Freeze Concentration Process, Chem. Eng. Trans. 56 (2017) 1147–1152.

[33] H. Shin, B. Kalista, S. Jeong, A. Jang, Optimization of simplified freeze desalination with surface scraped freeze crystallizer for producing irrigation water without seeding, Desalination. 452 (2019) 68–74.

[34] O. Miyawaki, S. Kato, K. Watabe, Yield improvement in progressive freeze-concentration by partial melting of ice, J. Food Eng. 108 (3) (2012) 377–382.

[35] O.L.A. Flesland, Freeze Concentratton by Layer Crystallization, Dry. Technol. 13 (8–9) (1995) 1713–1739.

[36] M. Gunathilake, M. Dozen, K. Shimmura, O. Miyawaki, An apparatus for partial ice-melting to improve yield in progressive freeze-concentration, J. Food Eng. 142 (2014) 64–69.

[37] C.M. Robles, M.X. Quintanilla-Carvajal, F.L. Moreno, E. Hernández, M. Raventós, Y. Ruiz, Ice morphology modification and solute recovery improvement by heating and annealing during block freeze-concentration of coffee extracts, J. Food Eng. 189 (2016) 72–81.

[38] F.L. Moreno, M.X. Quintanilla-Carvajal, L.I. Sotelo, C. Osorio, M. Raventós, E. Hernández, Y. Ruiz, Volatile compounds, sensory quality and ice morphology in falling-film and block freeze concentration of coffee extract, J. Food Eng. 166 (2015) 64–71.

[39] M. Hasan, N. Rotich, M. John, M. Louhi-Kultanen, Salt recovery from wastewater by air-cooled eutectic freeze crystallization, Chemical Engineering Journal 326 (2017) 192–200.

[40] M. Hasan, M. Louhi-Kultanen, Ice growth kinetics modeling of air-cooled layer crystallization from sodium sulfate solutions, Chem. Eng. Sci. 133 (2015) 44–53.

[41] A. Ojeda, F.L. Moreno, R.Y. Ruiz, M. Blanco, M. Raventós, E. Hernández, Effect of Process Parameters on the Progressive Freeze Concentration of Sucrose Solutions, Chem. Eng. Commun. 204 (8) (2017) 951–956.

[42] X. Yu, J. Wang, J. Ulrich, Purification of Lysozyme from Protein Mixtures by Solvent-Freeze-Out Technology, Chem. Eng. Technol. 37 (8) (2014) 1353–1357.

[43] O. Flesland, Freeze Concentratton by Layer Crystallization, Dry. Technol. 13 (1995) 1713–1739.

[44] M. John, M. Suominen, E. Kurvinen, M. Hasan, O.-V. Sormunen, P. Kujala, A. Mikkola, M. Louhi-Kultanen, Separation efficiency and ice strength properties in simulated natural freezing of aqueous solutions, Cold. Reg. Sci. Technol. 158 (2019) 18–29.

[45] K. Nakagawa, H. Nagahama, S. Maebashi, K. Maeda, Usefulness of solute elution from frozen matrix for freeze-concentration technique, Chemical Engineering Research and Design 88 (5) (2010) 718–724.

[46] F.L. Moreno, C.M. Robles, Z. Sarmiento, Y. Ruiz, J.M. Pardo, Effect of separation and thawing mode on block freeze-concentration of coffee brews, Food and Bioproducts Processing 91 (4) (2013) 396–402.

[47] S.C. Sequera, Y. Ruiz, F.L. Moreno, M.X. Quintanilla-Carvajal, F. Salcedo, Rheological evaluation of gelation during thermal treatments in block freeze concentration of coffee extract, J. Food Eng. 242 (2019) 76–83.

[48] O. Miyawaki, M. Gunathilake, C. Omote, T. Koyanagi, T. Sasaki, H. Take, A. Matsuda, K. Ishisaki, S. Miwa, S. Kitano, Progressive freeze-concentration of apple juice and its application to produce a new type apple wine, J. Food Eng. 171 (2016) 153–158.

[49] D. Nowak, E. Jakubczyk, The Freeze-Drying of Foods-The Characteristic of the Process Course and the Effect of Its Parameters on the Physical Properties of Food Materials, Foods. 9 (10) (2020).

[50] M. Hasan, M. Louhi-Kultanen, Water purification of aqueous nickel sulfate solutions by air cooled natural freezing, Chemical Engineering Journal 294 (2016) 176–184.

[51] T. Rashid, F. Sher, M. Jusoh, T.A. Joya, S. Zhang, T. Rasheed, E.C. Lima, Parametric optimization and structural feature analysis of humic acid extraction from lignite, Environ. Res. 220 (2023) 115160.

[52] D. Fu, G. Mazza, Optimization of processing conditions for the pretreatment of wheat straw using aqueous ionic liquid, Bioresour. Technol. 102 (17) (2011) 8003–8010.

[53] T. Rashid, N. Gnanasundaram, A. Appusamy, C.F. Kait, M. Thanabalan, Enhanced lignin extraction from different species of oil palm biomass: kinetics and optimization of extraction conditions, Ind. Crops. Prod. 116 (2018) 122–136.

[54] Z. Zhang, X.-Y. Liu, Control of ice nucleation: freezing and antifreeze strategies, Chem. Soc. Rev. 47 (18) (2018) 7116–7139.

[55] J.M. Auleda, M. Raventós, J. Sánchez, E. Hernández, Estimation of the freezing point of concentrated fruit juices for application in freeze concentration, J. Food Eng. 105 (2) (2011) 289–294.

[56] Q.-Q. Gai, F. Qu, Z.-J. Liu, R.-J. Dai, Y.-K. Zhang, Superparamagnetic lysozyme surface-imprinted polymer prepared by atom transfer radical polymerization and

its application for protein separation, Journal of Chromatography A 1217 (31) (2010) 5035–5042.
[57] R. Dembczyński, W. Białas, K. Regulski, T. Jankowski, Lysozyme extraction from hen egg white in an aqueous two-phase system composed of ethylene oxide–propylene oxide thermoseparating copolymer and potassium phosphate, Process Biochemistry 45 (3) (2010) 369–374.
[58] D.A. Omana, J. Wang, J. Wu, Co-extraction of egg white proteins using ion-exchange chromatography from ovomucin-removed egg whites, Journal of Chromatography B 878 (21) (2010) 1771–1776.
[59] G. Leśnierowski, R. Cegielska-Radziejewska, Potential possibilities of production, modification and practical application of lysozyme, Acta Sci. Pol. Technol. Aliment. 11 (3) (2012) 223–230.
[60] Yeh, A. Characterization of a novel weak cation-exchange hydrogel membrane through the separation of lysozyme from egg white. 2012.
[61] N.S. Abeyrathne, H.Y. Lee, D.U. Ahn, Sequential separation of lysozyme and ovalbumin from chicken egg white, Korean J. Food Sci. Anim. Resour. 33 (4) (2013) 501–507.
[62] E.D.N.S. Abeyrathne, H.Y. Lee, D.U. Ahn, Sequential separation of lysozyme, ovomucin, ovotransferrin, and ovalbumin from egg white, Poult. Sci. 93 (4) (2014) 1001–1009.
[63] Z. Wulandari, D. Fardiaz, C. Budiman, T. Suryati, D. Herawati, Purification of Egg White Lysozyme from Indonesian Kampung Chicken and Ducks, 38, Media Peternakan, 2015, pp. 18–26.
[64] M. Tagaya, S. Nagoshi, M. Matsuda, S. Takahashi, S. Okano, K. Hara, Hemodialysis membrane coated with a polymer having a hydrophilic blood-contacting layer can enhance diffusional performance, Int. J. Artif. Organs 40 (12) (2017) 665–669.
[65] A. Noraaini, H. Sofiah, A. Asmadi, M.Abdul Wahab, Preparation and Characterization of Asymmetric Ultrafiltration Membrane for Lysozyme Separation: effect of Polymer Concentration, J. Appl. Membrane Sci. Technology 11 (1) (2017).
[66] F. Yang, F. Tao, C. Li, L. Gao, P. Yang, Self-assembled membrane composed of amyloid-like proteins for efficient size-selective molecular separation and dialysis, Nat. Commun. 9 (1) (2018) 5443.
[67] S.M. Miron, P. Dutournié, K. Thabet, A. Ponche, Filtration of protein-based solutions with ceramic ultrafiltration membrane. Study of selectivity, adsorption, and protein denaturation, Comptes Rendus Chimie 22 (2) (2019) 198–205.